NATIONAL ADVISORY COMMITTEE FOR AERONAUTICS

TECHNICAL NOTE 4378

PRELIMINARY HEAT-TRANSFER STUDIES ON TWO BODIES OF REVOLUTION AT ANGLE OF ATTACK AT A MACH NUMBER OF 3.12

By Norman Sands and John R. Jack

Lewis Flight Propulsion Laboratory
Cleveland, Ohio

Washington

September 1958

NATIONAL ADVISORY COMMITTEE FOR AERONAUTICS

TECHNICAL NOTE 4378

PRELIMINARY HEAT-TRANSFER STUDIES ON TWO BODIES OF REVOLUTION AT ANGLE OF ATTACK AT A MACH NUMBER OF 3.12

By Norman Sands and John R. Jack

SUMMARY

Local rates of heat transfer were obtained for a cone-cylinder model and a parabolic-nosed-cylinder model at a Mach number of 3.12 and angles of attack up to 18°. Data were obtained for cooled surfaces at unit Reynolds numbers of 0.36 and 0.65 million per inch based on free-stream conditions. Zero angle of attack data are included for comparison.

For similar type boundary layers heat-transfer coefficients at angle of attack were always higher than those at zero angle of attack at corresponding geometric locations. On the windward side Stanton numbers increased steadily with angle of attack; however, no systematic variation of Stanton numbers with angle of attack was found on the sheltered side.

The parabolic forebody showed the following advantages over the conical forebody: (a) it increased the extent of laminar boundary layer on the windward side of the model, and (b) it reduced the Stanton numbers on corresponding geometric locations of the two models (when the models possessed similar type boundary layers), except on the leeward side where no definite advantage was evident due to forebody geometry.

Heat-transfer coefficients along the most windward and most leeward generators were approximately equal near the tip of the models at all test configurations. Toward the aft part of the models, however, the ratio of Stanton numbers along the most leeward to those along the most windward generators at equivalent distances from the tip was between 2 and 3 at 3° angle of attack, and gradually decreased to a ratio of approximately 1/2 at 18° angle of attack.

Within the range and accuracy of the investigation, the unit Reynolds number did not have a significant effect on the values of the Stanton numbers along the most leeward generator of both models.

INTRODUCTION

The problems associated with aerodynamic heating of an axisymmetric body at zero angle of attack have been extensively studied, both theoretically and experimentally. The problems involved, however, increase in complexity when the body is subjected to some angle of attack with respect to the undisturbed free stream.

Few theoretical attempts to solve the problem of a cone at angle of attack under heat-transfer conditions have been made up to the present time. The flow analyses available are limited to conditions that reduce the range of their applicability. Reference 1 is limited to isothermal wall conditions and only applies to the most windward generator, provided the boundary layer there is laminar. The same limitations of laminar boundary layer and isothermal wall conditions are required for the application of the theory of reference 2; it can be used to find the heat transfer along any generator of a cone, but is restricted to small angles of attack. In order to contribute to the experimental approach of these problems, the Lewis laboratory initiated in 1954 a series of tests designed to isolate and establish the effects of specific parameters on heat-transfer characteristics at angle of attack. All tests were conducted in the same wind-tunnel facility (see APPARATUS AND PROCEDURE) with the same bodies of revolution (see fig. 1).

In the early stages of this program, studies were made to find the effect of heat transfer and pressure gradient on the location of transition at zero angle of attack (ref. 3). In another report (ref. 4) heat-transfer data were presented for the two models of figure 1 at zero angle of attack. Reference 5 dealt with the effects of extreme cooling of these models on boundary-layer transition. The objective of previous tests at angle of attack was to find what effect it had on recovery factors (ref. 6).

This paper presents the effects of angle of attack on heat-transfer characteristics on a cone cylinder and parabolic-nosed cylinder (fig. 1). Included for comparison are the heat-transfer data on these models at zero angle of attack. Limitations on data accuracy due to testing techniques and an estimate of the maximum errors introduced by radiation and condition effects are included in the text.

APPARATUS AND PROCEDURE

The investigation was conducted in the Lewis 1- by 1-foot supersonic wind tunnel, which operates at a Mach number of 3.12. Tests were made at two values of the unit Reynolds number, namely, 0.36 and 0.65 million per inch. The tunnel stagnation dew point was about -35° F at all times. Further details concerning this facility may be found in reference 3.

The dimensions and thermocouple locations of the models used to obtain the heat-transfer data are shown in figure 1. Both models were constructed from a nickel alloy with a wall thickness of approximately 1/16 inch. The cone cylinder was made of monel, whereas the parabolic-nosed cylinder was fabricated from "K" monel. The maximum surface roughness on each was less than 16 microinches. Each model was instrumented with calibrated copper-constantan thermocouples of 30-gage wire. Axial temperature distributions for both models were determined from three rows of 15 thermocouples each, located on three axial planes (generators) at 45 meridional degrees apart. The test models were first cooled to 120° R by enclosing them in a set of shoes, figure 2(a), and by passing liquid nitrogen into the shoes and over the model surface. The nitrogen was then exhausted through the base of the shoes. Photographs of the cone-cylinder model with shoes along the tunnel wall and in place are given in figures 2(a) and (b), respectively.

The shoes could be operated while the tunnel was running. For any given test, the shoes were placed over the model after the desired tunnel conditions had been reached. The model was then precooled by passing liquid nitrogen through the retraction struts. After a uniform wall temperature of 120° R was obtained, the shoes were snapped back against the tunnel walls by means of air cylinders (fig. 2(b)).

Heat-transfer data were obtained by utilizing the transient technique described in detail in reference 3. Transient temperature distributions were obtained from data recorded on multichannel oscillographs.

The flow over a body of revolution at angle of attack is essentially symmetric about a plane containing the most windward and most leeward generators. The greatest deviation from symmetry about this plane would be anticipated in the separated flow region of the sheltered side. Because of the essentially symmetrical flow, only half of the parabolic-nosed-cylinder model located entirely on one side of the plane of symmetry was investigated. Data at a given angle of attack were obtained in two installments. The parabolic-nosed-cylinder model was first mounted in the tunnel at an angle of attack α with its three rows of thermocouples occupying the 0° (most windward), 45°, and 90° generator locations. Later the model was placed in a $-\alpha$ position without rotation about its own axis; in this position the same three rows of thermocouples occupied the 180° (most leeward), 135°, and 90° generator locations, respectively. Thus, for each angle, data on the 90° generator of the parabolic-nosed-cylinder model were obtained twice. This duplication was intended to show the degree of repeatability of the test results. As seen from part (b) of tables II to V, the two sets of Stanton numbers obtained along this generator were within ±15 percent of their mean value for all test configurations.

With the cone-cylinder model data were obtained not only for the 0°, 45°, 90°, 135°, and 180° generator locations as with the parabolic-nosed cylinder model, but also along the 225° generator location on the other side of the plane of symmetry. This was accomplished by first obtaining data along the 0°, 45°, and 90° generator locations as previously described for the $+\alpha$ position. In placing the model at a $-\alpha$ position, it was also rotated 45° about its own axis so that the 0°, 45°, and 90° generator locations now occupied the 225°, 180°, and 135° positions, respectively. This modification was made in order to compare the heat-transfer results in regions symmetrically located about the plane of symmetry of the flow, when the flow is locally separated. The maximum deviation of Stanton numbers along the 135° and 225° generators was ±19 percent of their mean value (see part (a) of tables II to V). This is probably due to a combination of experimental inaccuracies and asymmetry of the flow on the sheltered side (see, e.g., ref. 6).

DATA REDUCTION

The general equation describing the transient heat-transfer process for a nonisothermal cone at angle of attack having a thin wall is

$$q_{measured} = q_{convection} + q_{\substack{conduction \\ in\ skin}} + q_{radiation} + q_{\substack{conductions\ to \\ inside\ of\ model}}$$

or more explicitly, in conical coordinates,

$$\rho_b c_{p,b} \tau \frac{\partial T_w}{\partial t} = h(T_{ad} - T_w) + k_b \tau \left(\frac{\partial^2 T_w}{\partial x^2} + \frac{1}{x} \frac{\partial T_w}{\partial x} + \frac{1}{x^2 \sin^2 \varphi} \frac{\partial^2 T_w}{\partial \theta^2} \right) + q_{radiation} + q_{\substack{conduction\ to \\ inside\ of\ model}} \tag{1}$$

where

$$T_w \equiv T_w(x, \theta, t)$$

(All symbols are defined in the appendix).

When the heat-transfer rates by radiation and conduction are small compared with those by convection, equation (1) gives the following expression for the local heat-transfer coefficient

$$h = \frac{\rho_b c_{p,b} \tau \frac{\partial T_w}{\partial t}}{T_{ad} - T_w} \tag{2}$$

Experimental values of h were determined by equation (2), and corresponding values of Stanton numbers based on properties of the undisturbed air ahead of the shock were computed from

$$St_o = \frac{h}{\rho_o c_{p,o} u_o} \tag{3}$$

Wall temperatures were computed for 15 seconds after the models were exposed to the main stream (by retracting the shoes). The exact choice of 15 seconds was somewhat arbitrary, but was made because of large temperature potentials ($T_{ad} - T_w$) and large rates of change of temperature with time ($\partial T_w/\partial t$) that existed at approximately 15 seconds, which would contribute to greater accuracy in reducing the data. Wall temperatures as $t \to \infty$ (when thermal equilibrium was reached) were used in lieu of adiabatic wall temperatures (T_{ad}) derived from a knowledge of the free-stream conditions and the recovery factor. The substitution of $T_{t\to\infty}$ for T_{ad} was made because of inaccurate knowledge of the numerical values of the recovery factors in the transitional phase between laminar to turbulent boundary layers, and, especially in regions of crossflow separation. Some of the experimental equilibrium wall temperatures obtained in this way might be as much as 14° F too high in regions where laminar boundary layer existed at 15 seconds and then became turbulent upon reaching equilibrium conditions. In such regions the actual values of the Stanton numbers might be up to 7 percent higher than the values listed in tables I to V since the laminar boundary-layer regions that existed at 15 seconds had an average temperature potential ($T_{ad} - T_w$) of about 200° F.

An additional effect of substituting $T_{t\to\infty}$ for T_{ad} was that heat conduction within the model material (see below) caused the equilibrium temperatures to differ somewhat from their corresponding true adiabatic temperatures, thus introducing an added error in the computations. In regions where the boundary layer remained either laminar or turbulent during the entire duration of the test, the maximum difference between $T_{t\to\infty}$ and T_{ad} was 8° F, which, for the average temperature potential ($T_{ad} - T_w$) of 200° F, amounted to a maximum Stanton number error of ± 4 percent.

Time rates of change of temperature were found by using five data points: T_{15} (the temperature at 15 sec), $T_{15\pm\delta}$, and $T_{15\pm 2\delta}$ where δ is a time increment. A quadratic curve was then fitted through these points by the method of least squares, and a slope of this curve evaluated at T_{15}.

The following are the estimated uncertainties of the basic quantities:

Wall thickness, τ, percent	± 1
Slope $\partial T_w/\partial t$, percent	± 3
Specific heat of model wall material, $c_{p,b}$, percent	± 3
Model wall temperature, $^{\circ}R$	± 2
Model equilibrium wall temperature, $^{\circ}R$	± 2
Tunnel total temperature, $^{\circ}R$	± 2
Tunnel total pressure, percent	± 0.3

The errors introduced in neglecting the radiation and axial conduction terms in equation (1) were investigated in reference 4 for a cone at zero angle of attack and were less than 2 percent of the total heat absorbed. With the model at angle of attack the errors due to radiation and axial conduction are essentially the same as those for zero angle of attack. An additional source of error is, however, involved at angle of attack, namely, peripheral heat conduction within the model material.

The peripheral heat conduction for a thin-walled cone at angle of attack is given by (see eq. (1))

$$q_{\substack{\text{peripheral}\\ \text{conduction}}} = k_b \tau \frac{1}{x^2 \sin^2\varphi} \frac{\partial^2 T_w}{\partial \theta^2} \tag{4}$$

where

$$T_w \equiv T_w(x, \theta, t)$$

In order to estimate the error involved by neglecting this term in evaluating the convective heat-transfer coefficient (eq. (2)), it is necessary to compare the amount of heat conducted along the periphery of the cone (eq. (4)) with the measured amount of heat influx ($q_{measured}$, eq. (1)). However, not enough peripheral temperature-distribution data were available to determine $\partial^2 T_w/\partial \theta^2$ with reasonable accuracy. An alternative approach was, therefore, taken to estimate this effect by comparing Stanton numbers obtained at $t = 15$ seconds (when conduction was present) with those obtained at $t \sim 0$ second (when the wall temperature was essentially uniform so that conduction was very small). This comparison was made only for the most windward generator of the conical forebody and is discussed in detail in RESULTS AND DISCUSSION. Unfortunately, it was not possible to analyze all the data for the zero time condition where conduction errors would automatically be eliminated. The existence of transition reversal (ref. 7) for some test conditions prevented the evaluation of all heat-transfer data at these very early times.

RESULTS AND DISCUSSION

Wall temperatures at 15 seconds (T_w), equilibrium temperatures (T_{ad}), and Stanton numbers for both models are listed in tables I to V.

Zero angle of attack data are listed in tables I(a) and (b) for unit Reynolds numbers of 0.36 and 0.65 million per inch, respectively. For the models at angle of attack the data are tabulated along generators. Tables II(a), III(a), IV(a), and V(a) list the data for the cone-cylinder model at 3°, 7°, 12°, and 18° angle of attack for both values of the unit Reynolds number, respectively. Corresponding data for the parabolic-nosed-cylinder model are given in tables II(b), III(b), IV(b), and V(b).

The discussion of the test results will, of course, pertain to the wall-to-free-stream temperature ratios for which the data were reduced.

Comparison with Theory

Experimental data along the most windward generator of the conical forebody are compared in figure 3 with the theories of references 1 and 2. As shown in figure 3, the data agree within 30 percent with the theory described in reference 1 at all angles of attack and within about the same percentage with the theory of reference 2 for 3° angle of attack.

The difference between theory and experiment as seen in figure 3 is probably the result of a combination of the following contributing factors.

Peripheral conduction: In order to evaluate the effect of peripheral conduction, Stanton numbers were evaluated at $t \sim 0$ (when conduction was quite small) and compared with corresponding Stanton numbers at $t = 15$ seconds (when large peripheral conductions probably existed). This was done along the most windward generator (where peripheral conduction would be largest) of the conical forebody at a unit Reynolds number of 0.36×10^6 per inch, and is shown in figure 4. This plot shows that peripheral conduction lowered the Stanton numbers by as much as 10 to 35 percent, but did not alter the general trend of increased Stanton number with angle of attack (compare figs. 4(e) and (f)).

Nonisothermal conditions: Experimental data were compared with isothermal theories when in reality definite temperature gradients existed both axially and circumferentially. Although no method is presently available to modify the isothermal theories to fit the present situation, there is strong evidence that the nonisothermal condition might substantially alter the theoretical isothermal heat-transfer coefficients (see ref. 8).

Uncertainties in application of theory: Within the range of "large angles of attack" (up to 8°) the theory developed in reference 1 solves the problem of a yawed circular cone. For "very large angles of attack" (from 12° up) a yawed infinite circular cylinder was substituted to approximate the cone at angle of attack. There would, therefore, be some doubt of the validity of the theoretical lines at 12° and 18° angle of attack in figure 3. Also, the theory of reference 2 is only valid in the limiting case of "vanishing" angles of attack. There is then a doubt whether 3° is small enough to be considered "vanishing", thereby affecting a meaningful comparison between the theory of reference 2 and the present experimental data (fig. 3(b)). In fact, since references 1 and 2 solve the same set of equations for the most windward generator of a cone at angle of attack, the difference between the two theoretical lines shown in figure 3(b) can only be attributed to the fact that in reference 2 only the first order term in angle of attack was retained, whereas both the first and second order terms were retained in the theory of reference 1. The data in figure 3(b) should therefore compare more appropriately with the theory of reference 1 than with that of reference 2 although neither theory can be employed as a direct comparison with experimental data because of the peripheral conduction and nonisothermal conditions mentioned before.

Effect of Angle of Attack

The effect of angle of attack on the heat-transfer coefficient along the most windward generator at a unit Reynolds number of 0.36 million per inch is shown in figure 5. Stanton numbers for both the cone-cylinder model, figure 5(a), and the parabolic-nosed-cylinder model, figure 5(b), increased with angle of attack. The abrupt increase in Stanton number at the aft part of the cone-cylinder model at 18° angle of attack, figure 5(a), is believed to be due to transition from laminar to turbulent boundary-layer flow.

Similar trends were obtained at the higher unit Reynolds number except for transition which appeared at both the 12° and 18° angle-of-attack configurations. At 12° attitude transition along the most windward generator of the cone-cylinder model was located at about 4 inches from the tip (see fig. 9(a)), whereas at 18° angle-of-attack transition had moved upstream to about $2\frac{1}{2}$ inches from the tip (fig. 9(b)).

It should be noticed that the transition locations shown in figures 5(a), 9(a) and (b) are associated with the wall-to-free-stream temperature ratios given in tables IV and V and also that transition would probably be located elsewhere for different temperature ratios.

A typical effect of angle of attack on heat-transfer coefficient along the most leeward generator is shown in figure 6. Contrary to the gradual increase in Stanton number with angle of attack observed along the most windward generators (fig. 5), heat-transfer coefficients along the most leeward generators (where the crossflow component was probably separated) appear to have no orderly pattern. Comparison of the data along the most leeward generator with corresponding data at zero angle of attack shows that the Stanton numbers at angle of attack are always higher than at zero angle of attack for corresponding test conditions and distances from the tip of the models, as seen in figure 6 for the particular cases shown. The latter effect applies also along all other generators for all test configurations.

Perhaps the most striking effect of angle of attack on the leeward side is the relatively high value of the heat-transfer coefficients near the aft part of the model at fairly small angles of attack as compared with those at zero angle of attack. This is readily seen by comparing the zero and the 3° angle-of-attack curves in figure 5 with those in figure 6. This effect is further illustrated in figure 7 where the Stanton numbers along the most windward and most leeward generators of the parabolic-nosed-cylinder model are shown at several angles of attack; also included for comparison in figure 7 are the data for the model at zero angle of attack. At the aft part of the model, ratios of Stanton numbers along the most leeward to those along the most windward generator were of the order of 2 to 3 at 3° angle of attack (see fig. 7(a)). This ratio decreased with increased angle of attack, figures 7(b) and (c), to a value of about 1/2 at 18° angle of attack, figure 7(d). Results similar to those shown in figure 7 were also obtained for the cone-cylinder model.

In contrast to the large range of variation with angle of attack of Stanton number ratios along the aft part of the most leeward and most windward generators, heat-transfer coefficients along these generators were approximately equal near the tip of the models at all test configurations.

Effect of Forebody Geometry

From a heat-transfer point of view, the parabolic forebody had two advantages over the conical forebody.

For corresponding unit Reynolds numbers, angles of attack, and geometric location, Stanton numbers on the parabolic forebody were generally lower than those on the conical forebody, except on the leeward side where no definite advantage due to forebody geometry could be established. A typical case illustrating the reduction in Stanton number due to forebody geometry is illustrated in figure 8 for the models at 12° angle of attack and unit Reynolds number of 0.36 million per inch.

The favorable pressure gradient associated with the parabolic forebody delayed the start of transition to turbulent flow on the windward side of the parabolic-nosed-cylinder model as compared with that on the cone-cylinder model. This is illustrated in figure 9 for the most windward generator (which is also a streamline of the flow) where the beginning of transition is recognized from the start of the rise in Stanton number with increased distance along the generator.

Effect of Crossflow Separation

An additional observation can be made concerning heat-transfer coefficients along the most leeward generators of the two models.

In figure 10 Stanton numbers along the most leeward generators of the two models at 18° angle of attack were plotted against distance from the tip of the models for both values of unit Reynolds number. As shown in figure 10, Stanton numbers at the two values of the unit Reynolds number are nearly equal in magnitude and appear to fluctuate randomly about their average value. Similar plots made for the smaller angles of attack exhibited the same general trend. This would suggest that within the range and accuracy of the experiments the unit Reynolds number did not have a significant effect on the values of the Stanton numbers along the most leeward generators. It is believed that the insensitivity of the Stanton numbers to the free-stream unit Reynolds number is due to crossflow separation.

SUMMARY OF RESULTS

The following results were obtained from an investigation of the convective heat-transfer properties of two bodies of revolution at angles of attack up to 18° at a Mach number of 3.12.

1. Experimental laminar heat-transfer coefficients obtained along the most windward generators of the conical forebody were within 30 percent of the theoretical values of references 1 and 2. This difference was attributed to a combination of the following factors: (a) peripheral conduction in the model material, (b) differences in the nonisothermal data of the experiment with isothermal theories, (c) possible invalidity of the theories in the range of present test conditions, and (d) accuracy in collection and reduction of data.

2. For similar type boundary layers Stanton numbers at angle of attack were always higher than those of corresponding geometric location and test conditions at zero angle of attack.

3. Along the most windward generators Stanton numbers increased steadily with increased angle of attack, whereas no orderly variation of Stanton number with angle of attack was found along the most leeward generator.

4. Heat-transfer coefficients along the most windward and most leeward generators were approximately equal near the tip of the models at all test configurations. Towards the aft part of the models, Stanton numbers along the most leeward generators at 3° angle of attack were about 2 to 3 times larger than those at equivalent distances from the tip along the most windward generators. This ratio of Stanton numbers along the most leeward and most windward generators decreased with increased angle of attack, reaching a value of approximately 1/2 at 18° angle of attack.

5. The parabolic forebody tended to reduce the heat-transfer coefficients on the windward side and to increase the span of laminar boundary layer in comparison with the conical forebody.

6. The unit Reynolds number had an insignificant effect on the heat-transfer coefficients along the most leeward generator.

Lewis Flight Propulsion Laboratory
National Advisory Committee for Aeronautics
Cleveland, Ohio, July 25, 1958

APPENDIX - SYMBOLS

c_p specific heat at constant pressure, Btu/(lb)(^oR)

h local heat-transfer coefficient, Btu/(sec)(sq ft)(^oR)

k thermal conductivity, Btu/(ft)(sec)(^oR)

q heat-transfer rate, Btu/(sq ft)(sec)

Re Reynolds number, $Re = \frac{u_o}{\nu_o} x$

r distance of surface to centerline of model (fig. 1(b))

St dimensionless heat-transfer coefficient defined by eq. (3), Stanton number

T temperature, ^oR

t time, sec

u velocity, ft/sec

x axial distance measured from the tip of the model, ft

α angle of attack

θ peripheral angle (for the most windward generator $\theta = 0^o$)

ν kinematic viscosity, (sq ft)/sec

ρ density, lb/(cu ft)

τ wall thickness, ft

φ cone half angle

Subscripts:

ad adiabatic

b model material

o free stream ahead of shock

t free-stream total condition

w conditions at the wall

REFERENCES

1. Reshotko, Eli: Laminar Boundary Layer with Heat Transfer on a Cone at Angle of Attack in a Supersonic Stream. NACA TN 4152, 1957.

2. Fiebig, Martin: Laminar Boundary Layer on a Spinning Circular Cone in Supersonic Flow at a Small Angle of Attack. TN 56-532, Graduate School Aero. Eng., Cornell Univ., June 1956. (Contract AF-18(600)-1523.)

3. Jack, John R., and Diaconis, N. S.: Variation of Boundary-Layer Transition with Heat Transfer on Two Bodies of Revolution at a Mach Number of 3.12. NACA TN 3562, 1955.

4. Jack, John R., and Diaconis, N. S.: Heat-Transfer Measurements on Two Bodies of Revolution at a Mach Number of 3.12. NACA TN 3776, 1956.

5. Jack, John R., Wisniewski, Richard J., and Diaconis, N. S.: Effects of Extreme Surface Cooling on Boundary-Layer Transition. NACA TN 4094, 1957.

6. Raney, D. J.: Measurements of the Cross Flow Around an Inclined Body at a Mach Number of 1.91. Tech. Note Aero. 2357, British RAE, Jan. 1955.

7. Jack, John R., and Moskowitz, Barry: Experimental Investigation of Temperature Recovery Factors on a 10° Cone at Angle of Attack at a Mach Number of 3.12. NACA TN 3256, 1954.

8. Eckert, E. R. G., Hartnett, J. P., and Birkebak, Roland: Simplified Equations for Calculating Local and Total Heat Flux to Nonisothermal Surfaces. Jour. Aero. Sci., vol. 24, no. 7, July 1957, pp. 549-551.

TABLE I. - AXIAL TEMPERATURE AND STANTON NUMBER DISTRIBUTIONS AT ZERO ANGLE OF ATTACK.

(a) Cone-cylinder model.

x, in.	T_w, °R	T_{ad}, °R	Stanton number
T_t = 515° R; u_0/ν_0 = 0.366×10^6 in.$^{-1}$			
2	229	459	0.00104
3	212	458	.00085
4	199	461	.00072
5	189	462	.00058
6	184	468	.00046
7	173	465	.00041
8	182	471	.00040
9	180	471	.00039
10	176	471	.00036
10.62	176	469	.00029
11.5	170	471	.00022
12.5	168	469	.00020
13.62	170	470	.00021
14.75	168	470	.00017
16	164	468	.00019
T_t = 524° R; u_0/ν_0 = 0.646×10^6 in.$^{-1}$			
2	252	473	0.00082
3	235	477	.00065
4	218	481	.00053
5	206	480	.00042
6	192	482	.00036
7	196	480	.00034
8	204	481	.00035
9	202	480	.00033
10	198	480	.00030
10.62	209	480	-------
11.5	197	478	.00025
12.5	203	481	.00025
13.62	209	483	.00028
14.75	---	---	-------
16	213	481	.00033

(b) Parabolic-nosed-cylinder model.

x, in.	T_w, °R	T_{ad}, °R	Stanton number
T_t = 524° R; u_0/ν_0 = 0.360×10^6 in.$^{-1}$			
1	285	473	0.00175
1.5	256	471	.00115
2	238	471	.00090
3	216	469	.00071
4	208	470	.00063
5	195	468	.00049
6	189	470	.00041
7	183	468	.00038
8	178	470	.00033
9	173	471	.00028
10	170	474	.00023
11	170	479	.00022
12.5	166	485	.00023
14	171	480	.00023
16	174	479	.00022
T_t = 523° R; u_0/ν_0 = 0.649×10^6 in.$^{-1}$			
1	316	478	0.00130
1.5	285	476	.00089
2	265	476	.00072
3	240	474	.00054
4	233	478	.00045
5	223	476	.00036
6	221	483	.00032
7	216	485	.00028
8	212	487	.00025
9	213	485	.00022
10	212	485	.00022
11	219	485	.00022
12.5	221	486	.00027
14	237	484	.00037
16	266	482	.00050

4904

TABLE II. - AXIAL TEMPERATURE AND STANTON NUMBER DISTRIBUTIONS AT AN ANGLE OF ATTACK OF 3°.

(a) Cone-cylinder model.

x, in.	ϕ = 0°			ϕ = 45°			ϕ = 90°			ϕ = 135°			ϕ = 180°			ϕ = 225°		
	T_w, °R	T_{ad}, °R	Stanton number	T_w, °R	T_{ad}, °R	Stanton number	T_w, °R	T_{ad}, °R	Stanton number	T_w, °R	T_{ad}, °R	Stanton number	T_w, °R	T_{ad}, °R	Stanton number	T_w, °R	T_{ad}, °R	Stanton number
	T_t = 507° R; u_0/ν_0 = 0.354×10⁶ in.⁻¹									T_t = 521° R; u_0/ν_0 = 0.366×10⁶ in.⁻¹								
2	240	460	0.00140	228	461	0.00125	240	450	0.00114	242	472	0.00115	225	472	0.00112	241	473	0.00121
3	227	461	.00111	225	462	.00114	222	450	.00098	216	470	.00101	216	474	.00103	224	475	.00104
4	215	461	.00100	215	464	.00110	209	462	.00092	210	473	.00105	220	476	.00103	217	477	.00099
5	207	463	.00087	200	460	.00092	202	462	.00084	206	474	.00089	219	475	.00098	216	490	.00096
6	201	462	.00076	186	464	.00067	196	456	.00069	192	478	.00062	207	476	.00085	217	478	.00093
7	199	462	.00067	186	462	.00062	192	484	.00067	204	475	.00080	228	476	.00088	222	479	.00085
8	200	464	.00062	194	467	.00064	191	486	.00060	210	478	.00065	242	490	.00110	227	477	.00104
9	195	465	.00059	191	464	.00054	193	467	.00057	215	476	.00080	246	478	.00105	235	479	.00103
10	196	465	.00057	193	464	.00048	192	469	.00048	224	478	.00054	224	475	.00084	236	477	.00112
10.62	191	464	.00045	184	459	.00040	192	467	.00042	224	477	.00066	242	476	.00080	227	476	.00102
11.5	186	468	.00036	182	463	.00035	193	468	.00038	219	478	.00070	243	480	.00078	231	479	.00080
12.5	182	464	.00034	179	463	.00035	186	470	.00045	224	482	.00071	240	481	.00080	234	478	.00083
13.62	185	467	.00034	182	467	.00036	188	471	.00054	231	483	.00076	243	481	.00081	239	478	.00082
14.75	185	468	.00035	184	469	.00037	---	---	---	---	---	---	248	482	.00094	239	478	.00083
16	---	---	---	180	466	.00037	192	466	.00060	228	478	.00075	243	480	.00088	---	---	---
	T_t = 525° R; u_0/ν_0 = 0.649×10⁶ in.⁻¹									T_t = 521° R; u_0/ν_0 = 0.647×10⁶ in.⁻¹								
2	286	470	0.00107	266	476	0.00108	282	486	0.00108	284	477	0.00100	261	474	0.00109	254	476	0.00104
3	267	473	.00086	263	475	.00100	261	471	.00097	266	473	.00103	275	476	.00106	276	477	.00089
4	249	474	.00068	246	480	.00090	246	475	.00090	254	476	.00097	272	482	.00105	272	481	.00091
5	237	476	.00058	230	476	.00073	235	475	.00082	252	478	.00089	269	477	.00094	278	483	.00092
6	228	475	.00054	210	480	.00054	214	477	.00068	255	483	.00087	255	479	.00084	278	480	.00096
7	224	478	.00065	215	477	.00050	227	476	.00083	259	478	.00091	271	476	.00091	285	480	.00095
8	223	480	.00054	225	485	.00053	230	477	.00065	276	482	.00095	286	482	.00110	291	479	.00106
9	221	481	.00051	216	479	.00048	235	475	.00096	285	479	.00100	292	479	.00109	292	479	.00103
10	218	490	.00047	198	478	.00035	249	476	.00115	295	481	.00098	261	473	.00081	291	477	.00103
10.62	208	478	.00044	210	473	.00034	246	475	.00085	291	477	.00075	258	475	.00075	278	478	.00102
11.5	207	480	.00035	207	476	.00027	241	474	.00066	284	478	.00072	286	279	.00074	277	478	.00081
12.5	211	477	.00035	203	474	.00027	246	478	.00086	285	482	.00070	279	478	.00078	279	478	.00078
13.62	210	477	.00035	210	475	.00031	255	480	.00084	286	485	.00078	284	480	.00074	283	479	.00081
14.75	210	476	.00033	213	476	.00033	---	---	---	---	---	---	289	482	.00075	290	477	.00078
16	---	---	---	209	472	.00033	261	477	.00092	282	478	.00080	282	479	.00076	---	---	---

(b) Parabolic-nosed-cylinder model.

x, in.	ϕ = 0°			ϕ = 45°			ϕ = 90°			ϕ = 90°			ϕ = 135°			ϕ = 180°		
	T_w, °R	T_{ad}, °R	Stanton number	T_w, °R	T_{ad}, °R	Stanton number	T_w, °R	T_{ad}, °R	Stanton number	T_w, °R	T_{ad}, °R	Stanton number	T_w, °R	T_{ad}, °R	Stanton number	T_w, °R	T_{ad}, °R	Stanton number
	T_t = 506° R; u_0/ν_0 = 0.366×10⁶ in.⁻¹									T_t = 520° R; u_0/ν_0 = 0.368×10⁶ in.⁻¹								
1	---	---	---	---	---	---	283	459	0.00180	290	471	0.00180	---	---	---	---	---	---
1.5	268	461	.00133	260	457	.00138	255	457	.00130	260	471	.00126	250	471	.00112	254	473	.00135
2	250	459	.00110	244	459	.00103	241	459	.00112	245	472	.00108	233	475	.00106	228	472	.00084
3	233	460	.00084	222	455	.00088	218	460	.00091	221	472	.00074	206	472	.00065	212	476	.00078
4	224	461	.00085	217	460	.00075	210	465	.00075	213	476	.00067	---	477	---	217	479	.00093
5	---	---	---	214	457	.00080	197	460	.00080	205	472	.00054	188	476	.00055	222	479	.00088
6	207	461	.00062	204	453	.00054	192	458	.00042	196	478	.00048	181	481	.00059	223	480	.00086
7	202	464	.00049	193	460	.00045	186	465	.00040	190	475	.00040	183	479	.00048	231	479	.00086
8	195	459	.00044	190	461	.00040	181	467	.00038	185	477	.00034	190	479	.00047	---	---	---
9	187	459	.00041	187	462	.00035	177	467	.00034	182	477	.00051	182	477	.00050	232	478	.00080
10	185	461	.00040	184	464	.00035	173	466	.00031	178	478	.00031	188	485	.00051	229	479	.00078
11	189	462	.00043	184	465	.00038	172	467	.00033	175	481	.00033	191	479	.00054	238	480	.00082
12.5	---	---	---	---	---	---	174	468	.00038	175	483	.00037	---	---	---	---	---	---
14	---	---	---	182	468	.00046	---	---	---	---	---	---	218	480	.00078	---	---	---
16	---	---	---	---	---	---	184	465	.00048	183	479	.00046	---	---	---	---	---	---
	T_t = 510° R; u_0/ν_0 = 0.646×10⁶ in.⁻¹									T_t = 523° R; u_0/ν_0 = 0.649×10⁶ in.⁻¹								
1	---	---	---	---	---	---	313	461	0.00145	324	483	0.00135	---	---	---	---	---	---
1.5	295	465	.00110	239	462	.00101	281	462	.00106	291	481	.00095	287	480	.00103	290	485	.00108
2	275	462	.00081	271	465	.00078	267	465	.00092	276	484	.00079	271	483	.00091	280	484	.00088
3	255	463	.00064	245	462	.00057	244	466	.00071	252	487	.00068	252	483	.00084	287	487	.00092
4	245	465	.00060	238	457	.00052	234	471	.00059	243	491	.00066	264	490	---	301	492	.00104
5	---	---	---	226	455	.00045	222	467	.00050	235	486	.00063	279	483	.00119	309	487	.00104
6	227	468	.00044	226	472	.00059	216	469	.00049	229	492	.00059	282	487	.00116	306	487	.00100
7	222	469	.00038	215	469	.00038	210	468	---	223	487	.00055	276	486	.00105	301	485	.00094
8	215	468	.00035	213	470	.00032	209	470	.00055	220	488	.00056	278	485	.00082	---	---	---
9	209	470	.00030	207	466	.00030	217	469	.00076	221	487	.00064	277	485	.00082	297	485	.00084
10	204	468	.00030	205	467	.00026	223	467	.00083	219	486	.00071	278	484	.00076	289	484	.00080
11	209	470	.00031	204	466	.00026	235	469	.00092	228	488	.00083	279	485	.00073	294	485	.00082
12.5	---	---	---	---	---	---	248	469	.00096	248	496	---	---	---	---	---	---	---
14	---	---	---	214	468	.00041	---	---	---	---	---	---	292	484	.00080	---	---	---
16	---	---	---	---	---	---	280	465	.00096	285	482	.00101	---	---	---	---	---	---

TABLE III. - AXIAL TEMPERATURE AND STANTON NUMBER DISTRIBUTIONS AT AN ANGLE OF ATTACK OF 7°.

(a) Cone-cylinder model.

x, in.	θ = 0°			θ = 45°			θ = 90°			θ = 135°			θ = 180°			θ = 225°		
	T_w, °R	T_{ad}, °R	Stanton number	T_w, °R	T_{ad}, °R	Stanton number	T_w, °R	T_{ad}, °R	Stanton number	T_w, °R	T_{ad}, °R	Stanton number	T_w, °R	T_{ad}, °R	Stanton number	T_w, °R	T_{ad}, °R	Stanton number
	T_t = 506° R; u_0/ν_0 = 0.383×10⁶ in.⁻¹									T_t = 518° R; u_0/ν_0 = 0.370×10⁶ in.⁻¹								
2	261	461	0.00166	240	460	0.00150	256	459	0.00147	258	472	0.00140	243	471	0.00151	260	471	0.00157
3	247	461	.00121	238	462	.00125	235	457	.00130	244	470	.00133	244	473	.00128	242	471	.00123
4	235	463	.00116	225	462	.00125	217	459	.00117	221	470	.00120	235	476	.00114	231	473	.00107
5	227	462	.00100	212	458	.00105	208	460	.00097	213	472	.00100	228	478	.00095	227	476	.00109
6	221	461	.00085	197	463	.00077	198	463	.00073	197	475	.00074	218	476	.00076	218	474	.00091
7	219	462	.00082	204	460	.00078	193	459	.00073	207	473	.00080	231	474	.00095	225	475	.00098
8	217	461	.00072	206	464	.00077	194	462	.00073	212	478	.00081	251	481	.00122	228	477	.00090
9	216	462	.00073	208	462	.00075	192	463	.00065	215	477	.00086	252	479	.00106	230	479	.00087
10	208	461	.00068	185	460	.00054	191	466	.00055	216	480	.00088	224	476	.00076	228	479	.00094
10.62	199	460	.00063	203	458	.00048	191	466	.00059	215	477	.00068	240	475	.00078	216	478	.00085
11.5	199	461	.00052	200	461	.00046	179	468	.00037	204	479	.00061	243	479	.00080	217	481	.00063
12.5	198	458	.00045	200	462	.00041	177	467	.00036	201	482	.00062	238	479	.00079	219	479	.00073
13.62	204	460	.00047	203	462	.00049	181	470	.00043	206	482	.00071	243	479	.00079	218	480	.00070
14.75	203	463	.00048	202	466	.00045	---	---	-------	---	---	-------	254	481	.00091	224	480	.00061
16	---	---	-------	200	463	.00045	181	468	.00044	218	480	.00068	253	479	.00082	---	---	-------
	T_t = 516° R; u_0/ν_0 = 0.661×10⁶ in.⁻¹									T_t = 521° R; u_0/ν_0 = 0.648×10⁶ in.⁻¹								
2	299	467	0.00130	280	472	0.00111	295	464	0.00115	298	478	0.00117	278	474	0.00105	299	474	0.00133
3	261	468	.00111	278	470	.00106	270	465	.00105	272	473	.00092	284	477	.00115	2o3	475	.00103
4	265	470	.00096	261	473	.00107	248	469	.00108	256	477	.00102	276	482	.00115	274	479	.00107
5	254	470	.00082	242	471	.00080	236	470	.00094	252	479	.00089	274	479	.00105	272	482	.00107
6	248	471	.00069	223	474	.00084	218	474	.00089	234	484	.00081	255	481	.00080	270	482	.00101
7	245	471	.00060	230	473	.00057	232	472	.00085	261	475	.00103	275	490	.00084	278	482	.00098
8	242	475	.00053	241	479	.00060	239	474	.00086	277	484	.00101	301	487	.00116	285	485	.00098
9	240	475	.00054	235	476	.00055	248	473	.00093	280	482	.00096	298	483	.00119	289	485	.00095
10	235	476	.00052	213	475	.00043	266	473	.00110	289	484	.00090	292	479	.00083	283	483	.00090
10.62	228	479	.00048	225	470	.00045	266	472	.00062	284	480	.00088	285	479	.00078	269	483	.00088
11.5	225	478	.00038	225	475	.00041	248	471	.00074	272	481	.00055	286	482	.00071	263	483	.00066
12.5	227	475	.00038	220	472	.00040	249	473	.00080	267	488	.00067	290	482	.00071	284	483	.00068
13.62	233	474	.00037	227	470	.00044	253	476	.00084	272	486	.00072	288	483	.00066	286	484	.00066
14.75	229	471	.00036	231	472	.00043	---	---	-------	---	---	-------	296	484	.00085	285	482	.00067
16	---	---	-------	224	467	.00041	251	472	.00084	270	481	.00073	299	482	.00088	---	---	-------

(b) Parabolic-nosed-cylinder model.

x, in.	θ = 0°			θ = 45°			θ = 90°			θ = 90°			θ = 135°			θ = 180°		
	T_w, °R	T_{ad}, °R	Stanton number	T_w, °R	T_{ad}, °R	Stanton number	T_w, °R	T_{ad}, °R	Stanton number	T_w, °R	T_{ad}, °R	Stanton number	T_w, °R	T_{ad}, °R	Stanton number	T_w, °R	T_{ad}, °R	Stanton number
	T_t = 504° R; u_0/ν_0 = 0.385×10⁶ in.⁻¹									T_t = 518° R; u_0/ν_0 = 0.367×10⁶ in.⁻¹								
1	---	---	-------	---	---	-------	282	460	0.00180	292	471	0.00190	---	---	-------	---	---	-------
1.5	277	462	.00145	266	455	.00145	255	456	.00145	280	470	.00135	250	469	.00120	247	473	.00134
2	259	458	.00125	252	456	.00118	240	460	.00105	247	471	.00115	229	475	.00094	219	470	.00111
3	247	460	.00105	232	454	.00094	220	460	.00090	225	470	.00085	205	470	.00074	212	474	.00086
4	240	461	.00097	226	456	.00078	215	464	.00080	219	474	.00078	203	472	-------	221	478	.00088
5	---	---	-------	218	456	.00068	201	460	.00063	208	469	.00073	198	473	.00070	232	479	.00095
6	224	460	.00078	216	460	.00064	198	462	.00058	201	473	.00060	201	479	.00094	236	479	.00096
7	218	460	.00071	206	458	.00054	187	462	.00051	195	472	.00050	204	478	.00090	239	480	.00082
8	210	458	.00063	200	457	.00054	186	464	.00048	190	474	.00043	200	479	.00082	---	---	-------
9	204	457	.00060	198	459	.00047	182	465	.00044	188	474	.00040	200	478	.00068	239	478	.00067
10	200	459	.00057	197	462	.00041	177	464	.00041	181	474	.00040	201	481	.00075	234	479	.00063
11	200	459	.00065	195	461	.00053	175	467	.00041	181	478	.00040	202	481	.00068	241	481	.00068
12.5	---	---	-------	---	---	-------	176	467	.00041	186	481	.00040	---	---	-------	---	---	-------
14	---	---	-------	202	464	.00056	---	---	-------	---	---	-------	219	481	.00072	---	---	-------
16	---	---	-------	---	---	-------	181	464	.00043	187	479	.00038	---	---	-------	---	---	-------
	T_t = 509° R; u_0/ν_0 = 0.647×10⁶ in.⁻¹									T_t = 522° R; u_0/ν_0 = 0.648×10⁶ in.⁻¹								
1	---	---	-------	---	---	-------	320	462	0.00181	332	484	0.00150	---	---	-------	---	---	-------
1.5	309	466	.00120	301	461	.00120	290	481	.00111	300	482	.00110	294	482	.00115	300	488	.00113
2	292	465	.00088	285	465	.00093	278	464	.00085	289	485	.00100	277	487	.00097	286	487	.00105
3	275	465	.00083	265	463	.00078	258	467	.00085	286	488	.00089	272	488	.00124	294	488	.00107
4	286	466	.00076	257	469	.00072	258	472	.00088	261	491	.00062	283	488	-------	302	489	.00100
5	---	---	-------	243	467	.00057	255	468	.00094	256	487	.00075	287	486	.00094	303	488	.00092
6	250	467	.00061	246	471	.00054	254	470	.00094	254	488	.00083	294	489	.00100	298	488	.00088
7	244	467	.00054	234	469	.00049	286	469	.00091	252	487	.00089	285	487	.00087	292	486	.00077
8	234	466	.00048	227	469	.00044	251	471	.00085	251	488	.00091	282	487	.00086	---	---	-------
9	230	468	.00042	221	468	.00042	244	470	.00089	249	488	.00089	281	487	.00074	283	486	.00089
10	223	469	.00035	220	468	.00038	240	468	.00087	246	486	.00078	278	486	.00068	275	486	.00085
11	227	471	.00037	217	468	.00040	248	470	.00084	251	486	.00084	277	487	.00067	284	486	.00088
12.5	---	---	-------	---	---	-------	253	471	.00080	254	487	.00083	---	---	-------	---	---	-------
14	---	---	-------	226	467	.00045	---	---	-------	---	---	-------	275	487	.00068	---	---	-------
16	---	---	-------	---	---	-------	247	467	.00081	257	482	.00086	---	---	-------	---	---	-------

TABLE IV. - AXIAL TEMPERATURE AND STANTON NUMBER DISTRIBUTION AT AN ANGLE OF ATTACK OF 12°.

(a) Cone-cylinder model.

x, in.	ϕ = 0°			ϕ = 45°			ϕ = 90°			ϕ = 135°			ϕ = 180°			ϕ = 225°		
	T_w, °R	T_{ad}, °R	Stanton number	T_w, °R	T_{ad}, °R	Stanton number	T_w, °R	T_{ad}, °R	Stanton number	T_w, °R	T_{ad}, °R	Stanton number	T_w, °R	T_{ad}, °R	Stanton number	T_w, °R	T_{ad}, °R	Stanton number
	T_t = 506° R; u_0/ν_0 = 0.585×10⁶ in.⁻¹									T_t = 516° R; u_0/ν_0 = 0.569×10⁶ in.⁻¹								
2	273	456	0.00177	255	464	0.00161	263	452	0.00175	272	469	0.00181	251	470	0.00170	272	468	0.00155
3	255	458	.00151	251	460	.00126	239	456	.00150	245	466	.00141	249	470	.00145	248	466	.00132
4	245	456	.00130	236	462	.00131	220	459	.00127	227	466	.00125	227	472	-------	230	469	.00119
5	238	459	.00124	227	460	.00134	210	456	.00098	217	467	.00113	216	467	.00101	225	471	.00101
6	234	459	.00112	207	461	.00099	189	456	.00074	200	471	.00084	206	469	.00080	217	469	.00086
7	230	457	.00102	219	459	.00090	194	456	.00074	209	467	.00078	215	466	.00083	215	468	.00083
8	232	460	.00100	220	464	.00100	194	458	.00066	214	470	.00081	223	473	.00091	215	470	.00080
9	229	462	.00093	230	460	.00078	193	457	.00060	215	470	.00083	220	470	.00082	222	474	.00080
10	223	462	.00089	196	460	.00059	193	459	.00053	219	473	.00071	202	469	.00064	221	473	.00079
10.62	215	456	.00090	209	455	.00058	189	458	.00042	216	471	.00061	218	467	.00065	208	472	.00071
11.5	214	461	.00065	207	457	.00057	180	455	.00040	213	469	.00062	219	471	.00071	215	474	.00060
12.5	215	456	.00064	201	454	.00053	181	455	.00042	216	474	.00061	219	472	.00066	222	471	.00073
13.65	221	456	.00068	207	454	.00057	189	461	.00048	219	475	.00072	228	473	.00079	225	472	.00057
14.75	220	459	.00069	212	458	.00069	----	----	-------	----	----	-------	233	473	.00076	224	471	.00057
16	----	----	-------	207	454	.00066	191	462	.00060	222	472	.00076	227	470	.00077	----	----	-------
	T_t = 506° R; u_0/ν_0 = 0.843×10⁶ in.⁻¹									T_t = 522° R; u_0/ν_0 = 0.846×10⁶ in.⁻¹								
2	305	459	0.00145	278	462	0.00135	299	458	0.00138	306	476	0.00135	280	474	0.00125	307	475	0.00140
3	295	461	.00109	287	460	.00112	278	456	.00122	276	472	.00110	282	474	.00112	281	476	.00102
4	325	461	.00086	298	464	.00115	272	458	.00131	253	474	.00099	261	478	.00094	264	476	.00085
5	348	462	.00092	315	460	.00100	287	459	.00110	249	475	.00089	251	475	.00085	261	480	.00089
6	349	464	.00120	299	464	.00115	257	465	.00095	251	482	.00076	235	479	.00073	258	481	.00083
7	350	463	.00148	312	466	.00126	280	463	.00110	251	481	.00080	246	480	.00087	260	481	.00080
8	355	466	.00180	334	470	.00131	288	466	.00115	260	485	.00084	266	486	.00086	265	485	.00089
9	354	470	.00185	351	468	.00132	284	466	.00112	264	484	.00082	259	482	.00078	264	486	.00088
10	349	470	.00188	331	466	.00129	287	467	.00101	271	486	.00074	231	478	.00080	261	485	.00081
10.62	333	467	.00160	320	463	.00128	278	464	.00078	261	481	.00054	253	476	.00080	247	482	.00074
11.5	330	468	.00125	318	466	.00122	266	463	.00080	249	480	.00053	251	479	.00056	251	485	.00058
12.5	337	466	.00123	311	464	.00116	261	466	.00078	251	485	.00058	259	478	.00063	258	480	.00060
13.62	344	470	.00128	317	464	.00118	264	468	.00078	261	485	.00064	286	490	.00068	264	481	.00066
14.75	338	468	.00130	324	466	.00118	----	----	-------	----	----	-------	306	485	.00074	265	482	.00068
16	----	----	-------	315	462	.00118	258	467	.00076	262	485	.00072	301	481	.00085	----	----	-------

(b) Parabolic-nosed-cylinder model.

x, in.	ϕ = 0°			ϕ = 45°			ϕ = 90°			ϕ = 90°			ϕ = 135°			ϕ = 180°		
	T_w, °R	T_{ad}, °R	Stanton number	T_w, °R	T_{ad}, °R	Stanton number	T_w, °R	T_{ad}, °R	Stanton number	T_w, °R	T_{ad}, °R	Stanton number	T_w, °R	T_{ad}, °R	Stanton number	T_w, °R	T_{ad}, °R	Stanton number
	T_t = 514° R; u_0/ν_0 = 0.367×10⁶ in.⁻¹									T_t = 520° R; u_0/ν_0 = 0.362×10⁶ in.⁻¹								
1	----	----	-------	----	----	-------	307	468	0.00221	306	475	0.00225	----	----	-------	----	----	-------
1.5	300	470	.00175	288	467	.00180	275	465	.00158	275	472	.00156	265	472	.00145	270	476	.00148
2	285	467	.00145	272	467	.00140	259	467	.00139	261	474	.00130	246	474	.00115	246	472	.00118
3	266	466	.00124	247	463	.00121	234	466	.00108	256	472	.00106	222	470	.00091	242	474	.00084
4	260	465	.00117	245	465	.00108	224	467	.00091	227	475	.00090	----	478	-------	253	476	.00090
5	----	----	-------	232	463	.00086	210	462	.00071	214	469	.00074	207	470	.00073	257	475	.00087
6	247	468	.00102	229	467	.00092	201	464	.00070	207	470	.00072	209	474	.00070	256	476	.00094
7	240	466	.00089	219	462	.00076	197	463	.00061	201	469	.00061	202	471	.00060	255	476	.00090
8	230	464	.00078	215	462	.00070	193	463	.00048	196	471	.00052	201	473	.00058	----	----	-------
9	226	464	.00074	213	462	.00080	187	464	.00045	192	470	.00047	202	471	.00052	256	477	.00085
10	214	464	.00088	210	464	.00057	183	462	.00042	188	469	.00044	203	471	.00057	250	477	.00087
11	220	464	.00065	207	464	.00052	185	463	.00045	186	471	.00045	207	472	.00054	260	477	.00085
12.5	----	----	-------	----	----	-------	185	466	.00048	187	472	.00050	----	----	-------	----	----	-------
14	----	----	-------	213	465	.00054	----	----	-------	----	----	-------	219	473	.00063	----	----	-------
16	----	----	-------	----	----	-------	202	468	.00060	199	474	.00055	----	----	-------	----	----	-------
	T_t = 509° R; u_0/ν_0 = 0.646×10⁶ in.⁻¹									T_t = 522° R; u_0/ν_0 = 0.650×10⁶ in.⁻¹								
1	----	----	-------	----	----	-------	334	464	0.00170	354	490	0.00172	----	----	-------	----	----	-------
1.5	325	465	.00141	315	465	.00127	302	461	.00130	320	488	.00126	313	486	.00130	320	491	.00131
2	305	462	.00115	297	465	.00108	288	463	.00114	309	490	.00117	295	490	.00114	306	492	.00108
3	287	464	.00094	272	463	.00088	266	465	.00100	294	492	.00100	285	493	.00099	310	496	.00100
4	280	466	.00083	269	468	.00080	256	473	.00087	290	496	.00098	----	495	-------	316	497	.00101
5	----	----	-------	256	466	.00084	258	467	.00087	279	493	.00101	283	494	.00090	318	496	.00082
6	285	466	.00069	256	471	.00060	249	469	.00090	286	493	.00101	285	496	.00086	312	496	.00090
7	281	466	.00082	244	469	.00056	247	469	.00085	293	493	.00088	277	492	.00082	311	493	.00090
8	246	466	.00055	239	468	.00052	248	470	.00078	296	493	.00061	272	493	.00075	----	----	-------
9	251	466	.00054	235	467	.00048	240	469	.00071	292	492	.00077	265	493	.00067	309	494	.00084
10	244	469	.00049	228	467	.00046	225	468	.00063	282	490	.00075	280	493	.00058	306	494	.00085
11	248	469	.00048	225	467	.00044	218	469	.00057	279	490	.00074	261	494	.00065	321	494	.00088
12.5	----	----	-------	----	----	-------	217	472	-------	281	491	-------	----	----	-------	----	----	-------
14	----	----	-------	231	468	.00047	----	----	-------	----	----	-------	271	491	.00060	----	----	-------
16	----	----	-------	----	----	-------	255	470	-------	289	488	-------	----	----	-------	----	----	-------

TABLE V. - AXIAL TEMPERATURE AND STANTON NUMBER DISTRIBUTIONS AT AN ANGLE OF ATTACK OF 18°.

(a) Cone-cylinder model.

x, in.	θ = 0°			θ = 45°			θ = 90°			θ = 135°			θ = 180°			θ = 225°		
	T_w, °R	T_{ad}, °R	Stanton number	T_w, °R	T_{ad}, °R	Stanton number	T_w, °R	T_{ad}, °R	Stanton number	T_w, °R	T_{ad}, °R	Stanton number	T_w, °R	T_{ad}, °R	Stanton number	T_w, °R	T_{ad}, °R	Stanton number
	T_t = 506° R; u_0/v_0 = 0.365×10⁶ in.⁻¹									T_t = 515° R; u_0/v_0 = 0.367×10⁶ in.⁻¹								
2	282	455	0.00198	258	462	0.00184	274	451	0.00177	279	466	0.00180	255	466	0.00169	278	466	0.00198
3	288	456	.00161	257	452	.00162	269	453	.00155	246	482	.00152	245	464	.00140	249	464	.00148
4	260	456	.00145	245	460	.00153	229	455	.00155	224	464	.00148	223	466	.00115	226	464	.00118
5	261	458	.00136	239	458	.00140	219	452	.00108	213	463	.00104	210	462	.00081	217	467	.00099
6	258	458	.00130	226	461	.00117	198	454	.00075	197	467	.00077	195	464	.00069	207	465	.00086
7	257	458	.00120	229	457	.00100	207	454	.00081	202	464	.00063	201	462	.00064	206	465	.00082
8	261	460	.00116	246	462	.00105	209	455	.00087	207	467	.00070	216	466	.00072	203	466	.00087
9	261	463	.00110	241	459	.00102	207	454	.00088	207	466	.00076	214	464	.00072	202	467	.00056
10	257	464	.00105	218	460	.00074	210	456	.00054	207	467	.00064	193	460	.00060	200	465	.00062
10.62	248	459	.00085	235	454	.00078	208	456	.00050	208	464	.00043	214	461	.00059	194	464	.00058
11.5	248	463	.00078	234	456	.00074	196	452	.00050	204	464	.00044	213	463	.00058	200	465	.00047
12.5	248	457	.00076	230	454	.00067	195	451	.00045	207	466	.00047	209	465	.00060	200	465	.00038
13.62	257	461	.00087	236	455	.00070	202	451	.00049	211	471	.00053	215	466	.00069	209	467	.00054
14.75	356	472	.00255	299	462	.00190	---	---	---	---	---	---	239	470	.00100	244	465	.00087
16	---	---	---	427	465	---	334	450	.00280	269	457	.00150	285	463	.00149	---	---	---
	T_t = 508° R; u_0/v_0 = 0.641×10⁶ in.⁻¹									T_t = 522° R; u_0/v_0 = 0.648×10⁶ in.⁻¹								
2	298	460	0.00150	252	461	0.00170	290	460	0.00158	312	474	0.00185	284	474	0.00126	313	472	0.00180
3	306	462	.00140	287	480	.00158	265	458	.00148	276	470	.00120	279	476	.00118	280	472	.00112
4	345	462	.00200	311	464	.00190	261	460	.00160	251	472	.00103	257	477	.00086	259	474	.00093
5	359	466	.00228	319	461	.00200	272	460	.00156	242	473	.00082	244	475	.00074	254	477	.00080
6	367	466	.00240	300	465	.00155	251	467	.00107	225	478	.00068	224	478	.00064	242	484	.00068
7	373	468	.00250	325	466	.00180	275	465	.00115	237	476	.00072	234	475	.00063	243	478	.00071
8	379	471	.00270	352	474	.00209	292	468	.00115	248	481	.00067	257	482	.00074	247	482	.00072
9	377	472	.00265	348	470	.00200	290	468	.00110	250	481	.00068	254	478	.00067	248	483	.00070
10	375	472	.00255	298	468	.00152	290	468	.00099	256	482	.00067	253	476	.00054	248	481	.00064
10.62	367	470	.00243	337	467	.00142	275	465	.00080	250	479	.00049	251	473	.00052	256	481	.00061
11.5	384	471	.00190	337	468	.00135	283	464	.00076	247	478	.00050	256	478	.00052	244	482	.00042
12.5	359	466	.00197	328	466	.00135	259	467	.00078	252	484	.00054	257	479	.00055	251	481	.00056
13.62	367	471	.00196	337	467	.00145	286	470	.00083	260	486	.00059	273	480	.00060	261	482	.00056
14.75	372	471	.00200	390	468	.00158	---	---	---	---	---	---	290	481	.00065	266	481	.00066
16	---	---	---	445	472	---	360	448	.00190	309	457	.00119	321	468	.00128	---	---	---

(b) Parabolic-nosed-cylinder model.

x, in.	θ = 0°			θ = 45°			θ = 90°			θ = 90°			θ = 135°			θ = 180°		
	T_w, °R	T_{ad}, °R	Stanton number	T_w, °R	T_{ad}, °R	Stanton number	T_w, °R	T_{ad}, °R	Stanton number	T_w, °R	T_{ad}, °R	Stanton number	T_w, °R	T_{ad}, °R	Stanton number	T_w, °R	T_{ad}, °R	Stanton number
	T_t = 519° R; u_0/v_0 = 0.362×10⁶ in.⁻¹									T_t = 510° R; u_0/v_0 = 0.367×10⁶ in.⁻¹								
1	---	---	---	---	---	---	321	472	0.00251	318	483	0.00280	---	---	---	---	---	---
1.5	318	474	.00200	302	472	.00199	287	468	.00185	283	481	.00189	273	461	.00169	276	483	.00167
2	302	472	.00179	297	472	.00167	270	470	.00150	268	482	.00150	248	462	.00135	251	480	.00131
3	290	472	.00155	285	469	.00132	242	467	.00109	239	459	.00111	218	457	.00090	230	458	.00095
4	284	473	.00145	280	470	.00120	232	468	.00093	232	482	.00098	213	459	.00076	226	459	.00077
5	---	---	---	250	467	.00105	217	463	.00073	217	455	.00075	197	456	.00060	---	---	---
6	273	472	.00119	251	472	.00105	209	465	.00062	208	458	.00067	205	461	.00076	216	458	.00059
7	286	471	.00112	240	467	.00094	204	464	.00061	205	455	.00064	196	458	.00063	214	457	.00057
8	255	470	.00097	237	468	.00080	200	464	.00060	201	458	.00057	196	458	.00053	210	456	.00058
9	256	470	.00091	230	468	.00070	195	464	.00052	196	457	.00051	195	456	.00048	214	459	.00065
10	245	470	.00084	226	468	.00070	190	463	.00046	191	455	.00044	196	457	.00043	207	459	.00062
11	249	471	.00084	225	468	.00078	191	464	.00050	191	458	.00048	198	458	.00044	212	461	.00065
12.5	---	---	---	---	---	---	191	471	.00054	195	460	.00055	---	---	---	---	---	---
14	---	---	---	295	472	.00181	---	---	---	---	---	---	217	464	.00058	---	---	---
16	---	---	---	---	---	---	359	470	.00345	365	451	.00340	---	---	---	---	---	---
	T_t = 510° R; u_0/v_0 = 0.648×10⁶ in.⁻¹									T_t = 509° R; u_0/v_0 = 0.653×10⁶ in.⁻¹								
1	---	---	---	---	---	---	343	461	0.00200	350	463	0.00200	---	---	---	---	---	---
1.5	342	465	.00151	328	461	.00152	310	458	.00145	313	460	.00144	301	461	.00131	309	464	.00137
2	325	463	.00122	310	463	.00122	294	460	.00115	299	461	.00120	277	463	.00106	282	460	.00101
3	312	465	.00105	299	460	.00111	288	459	.00089	289	462	.00096	248	458	.00078	268	462	.00077
4	306	466	.00099	287	465	.00100	269	467	.00091	268	469	.00091	248	465	.00077	264	463	.00077
5	---	---	---	275	465	.00080	257	463	.00083	261	465	.00088	239	464	.00081	---	---	---
6	296	466	.00082	278	470	.00087	262	465	.00087	262	468	.00090	246	469	.00062	254	463	.00064
7	291	468	.00077	275	468	.00082	267	464	.00088	272	466	.00091	243	465	.00058	251	462	.00061
8	281	467	.00069	270	468	.00080	263	464	.00068	272	468	.00093	241	465	.00056	245	461	.00055
9	281	466	.00076	265	467	.00068	258	465	.00073	271	467	.00082	244	465	.00056	248	464	.00053
10	272	466	.00068	258	469	.00062	248	464	.00071	254	465	.00076	244	467	.00056	237	465	.00052
11	278	467	.00070	253	467	.00059	246	465	.00070	254	467	.00080	246	468	.00058	242	467	.00057
12.5	---	---	---	---	---	---	247	468	.00067	268	469	.00071	---	---	---	---	---	---
14	---	---	---	288	469	.00067	---	---	---	---	---	---	261	470	.00068	---	---	---
16	---	---	---	---	---	---	393	455	.00259	364	447	---	---	---	---	---	---	---

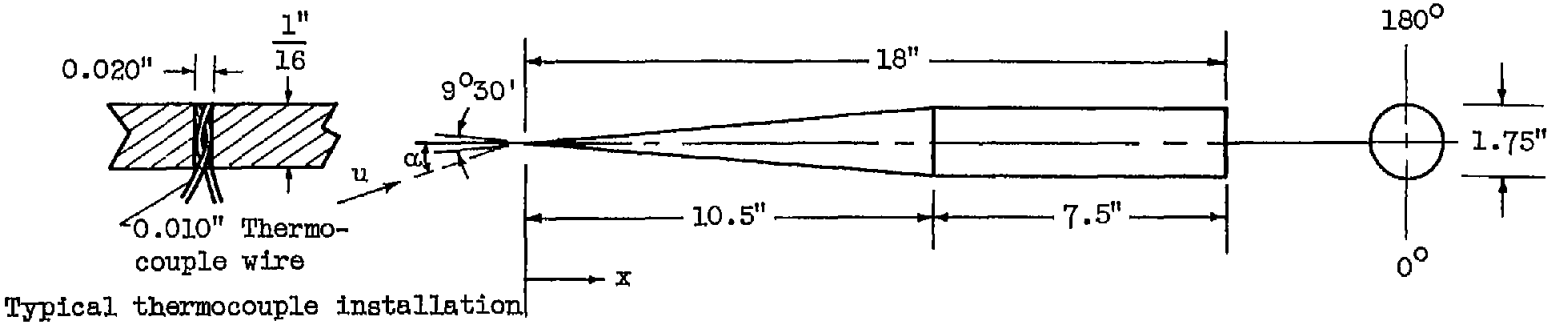

Thermocouple locations at axial distance, x, in.														
2.0	3.0	4.0	5.0	6.0	7.0	8.0	9.0	10.0	10.62	11.50	12.50	13.62	14.75	16.00

(a) Cone-cylinder model.

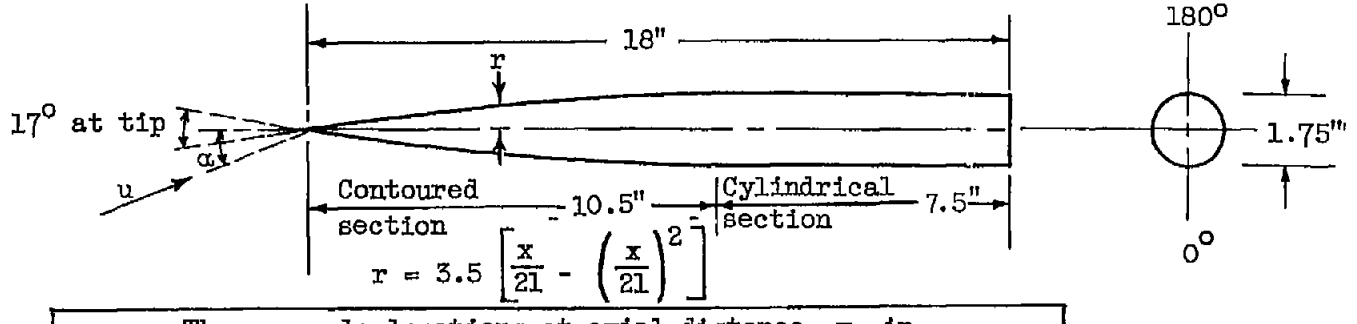

Thermocouple locations at axial distance, x, in.													
1.0	1.5	2.0	3.0	4.0	5.0	6.0	7.0	8.0	9.0	10.0	11.0	12.5	14.0	16.0

(b) Parabolic-nosed-cylinder model.

Figure 1. - Details of models and thermocouple locations.

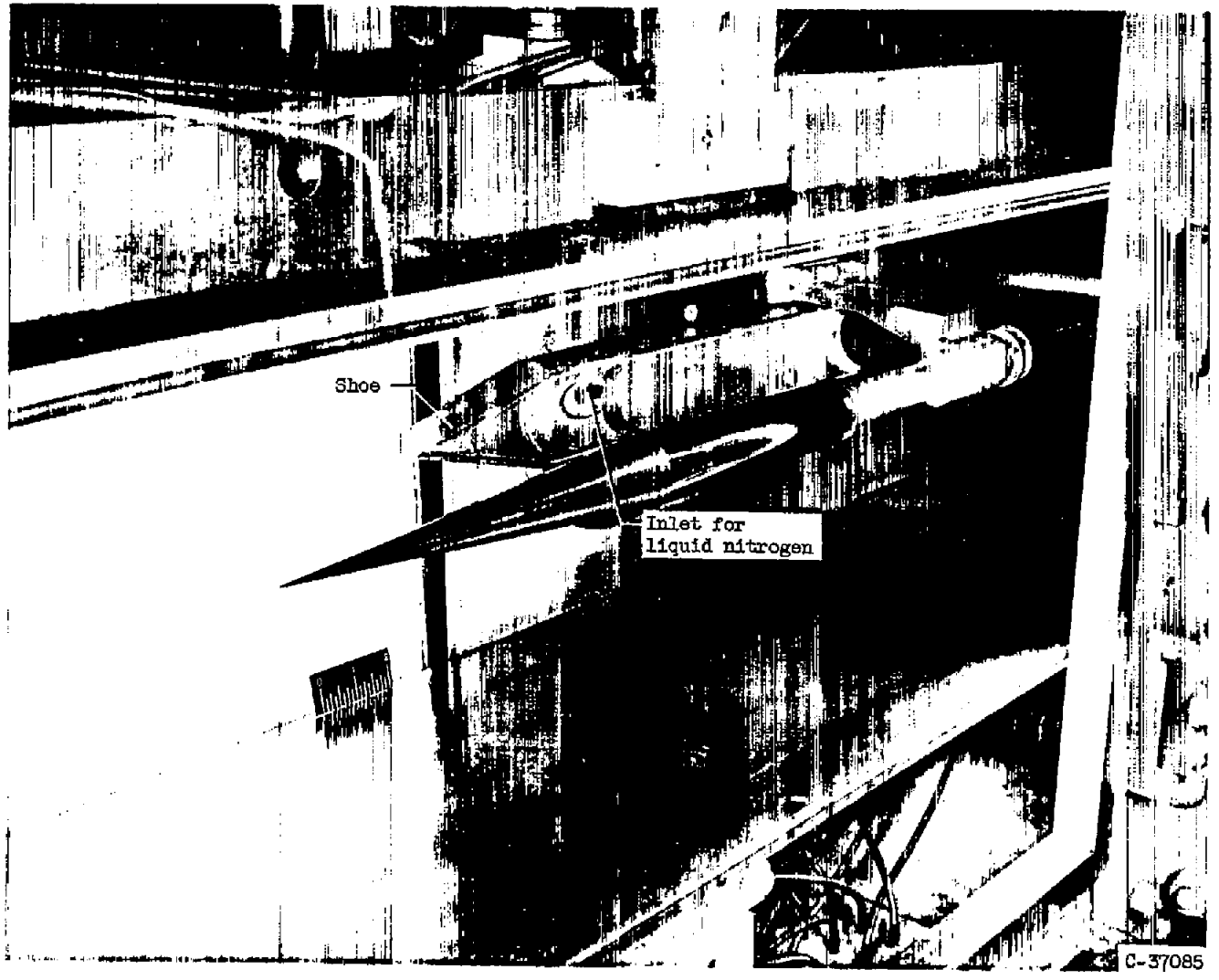

(a) Shoes in retracted position along the tunnel wall.

Figure 2. - Tunnel installation.

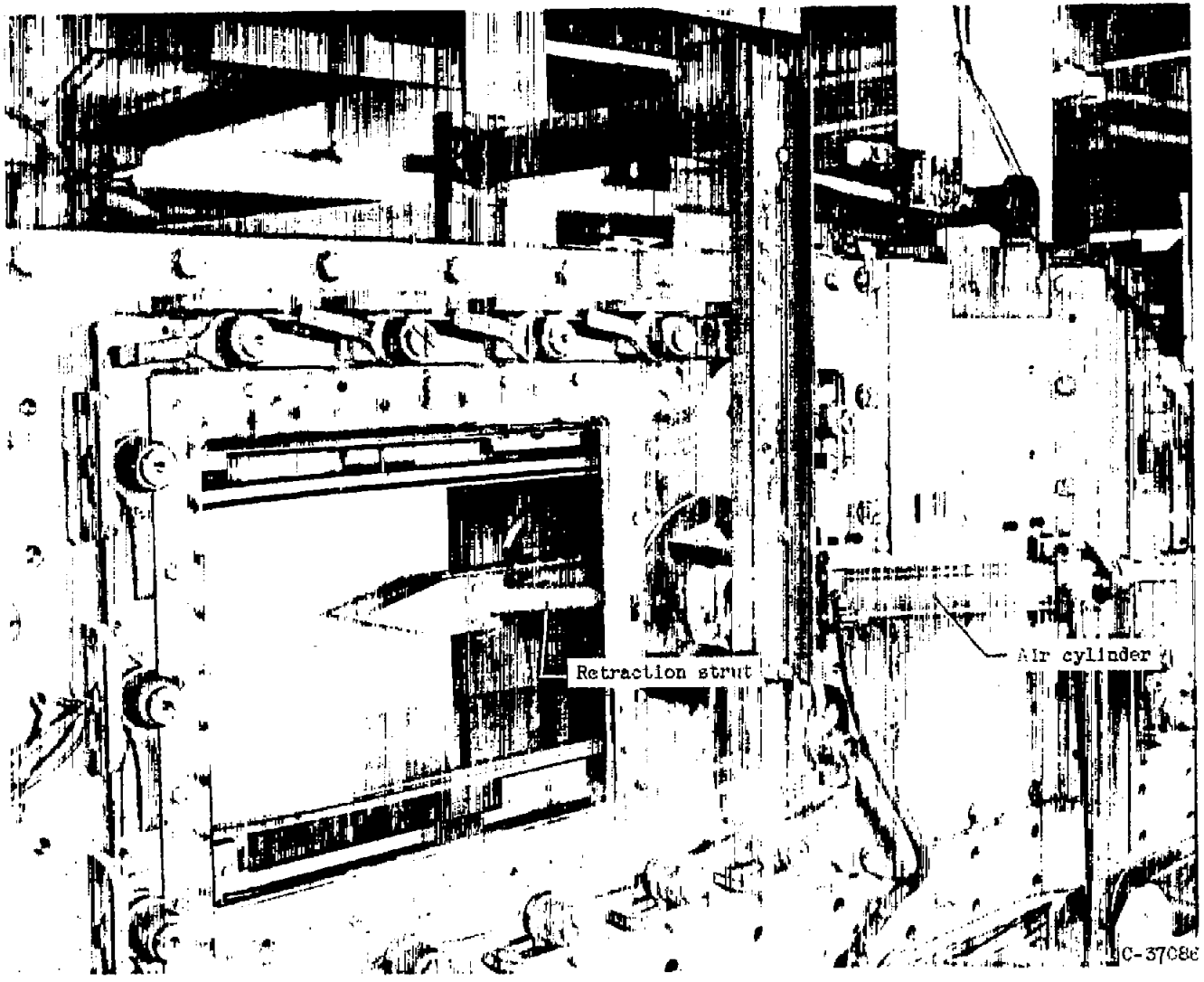

(b) Shoes enclosing model for precooling process.

Figure 2. - Concluded. Tunnel installation.

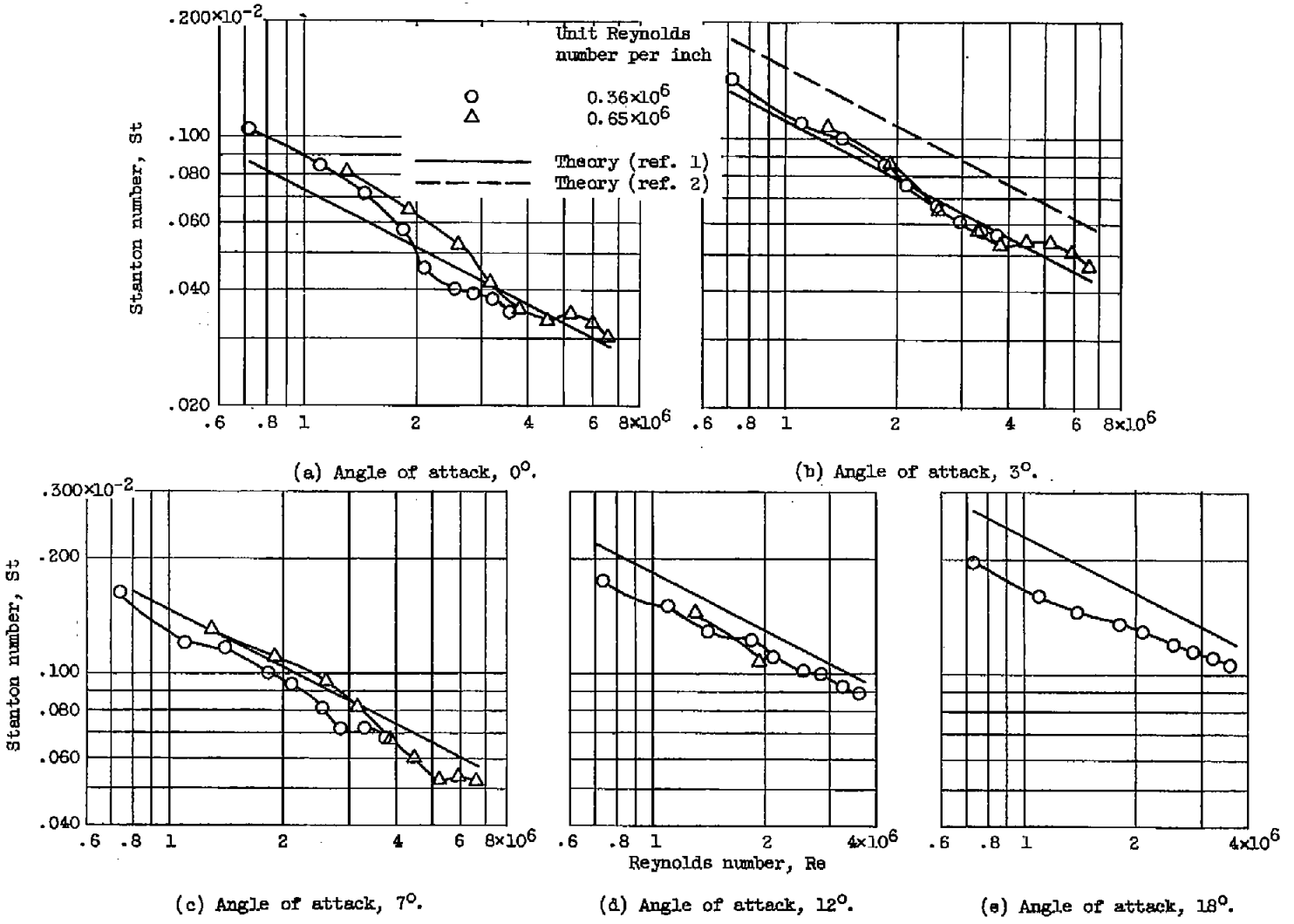

Figure 3. - Comparison of laminar boundary-layer theory with experimental data for the most windward (0°) generator of the conical forebody.

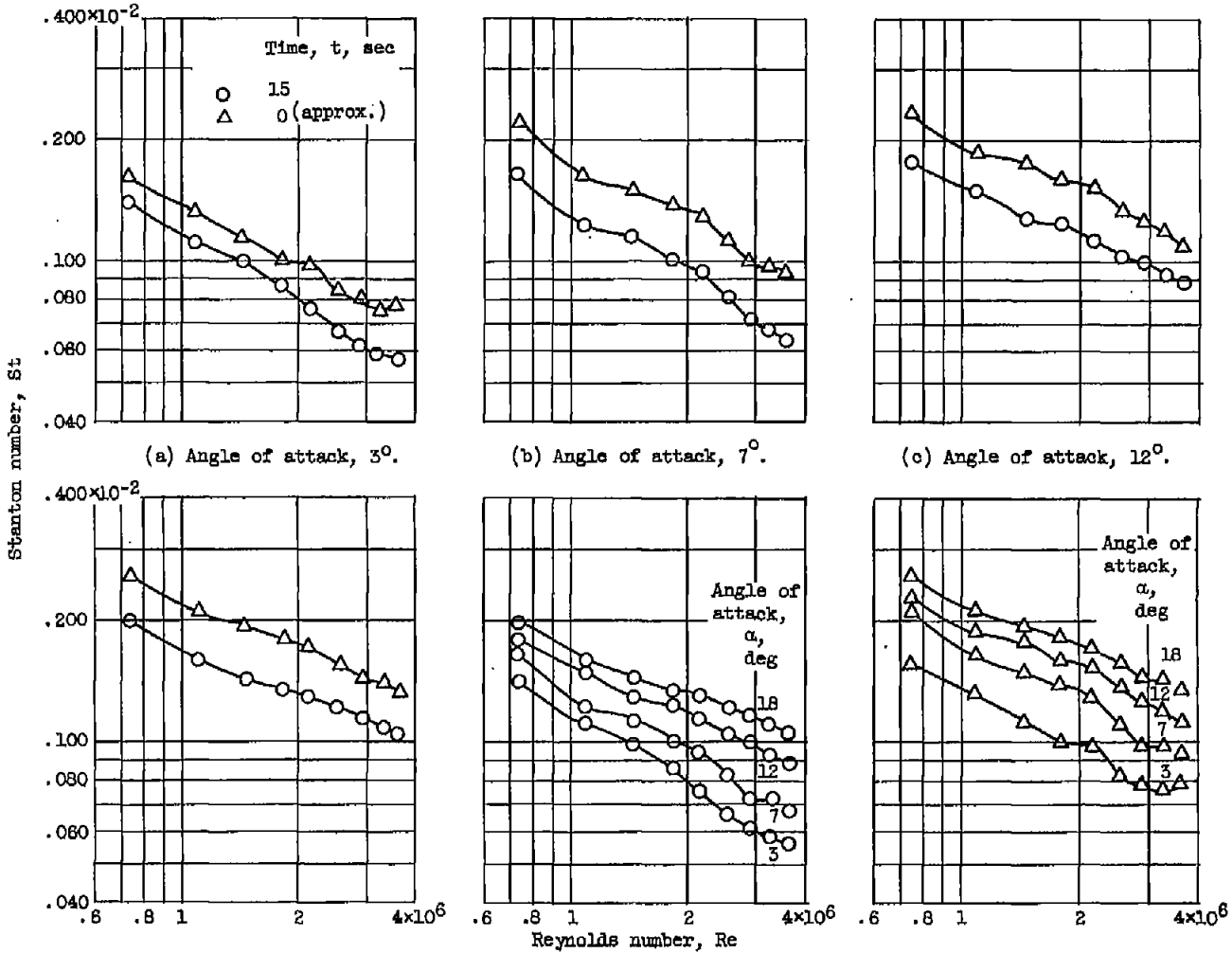

Figure 4. - Effect of peripheral conduction along the most windward generator of the conical forebody; unit Reynolds number per inch, 0.36×10^6.

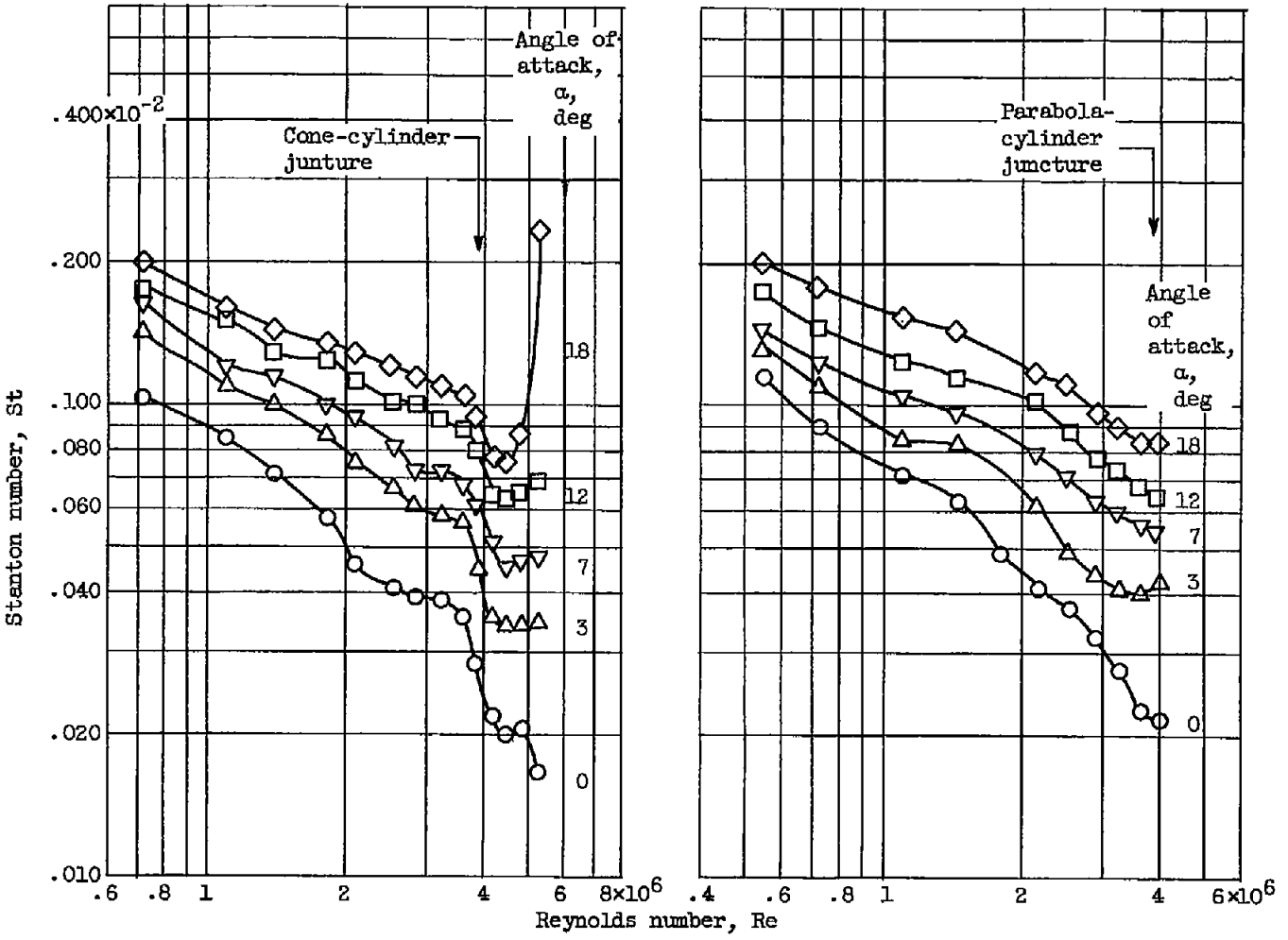

(a) Cone-cylinder model.

(b) Parabolic-nosed-cylinder model.

Figure 5. - Effect of angle of attack on heat-transfer coefficients along the most windward (0°) generator; unit Reynolds number per inch, 0.36×10^6.

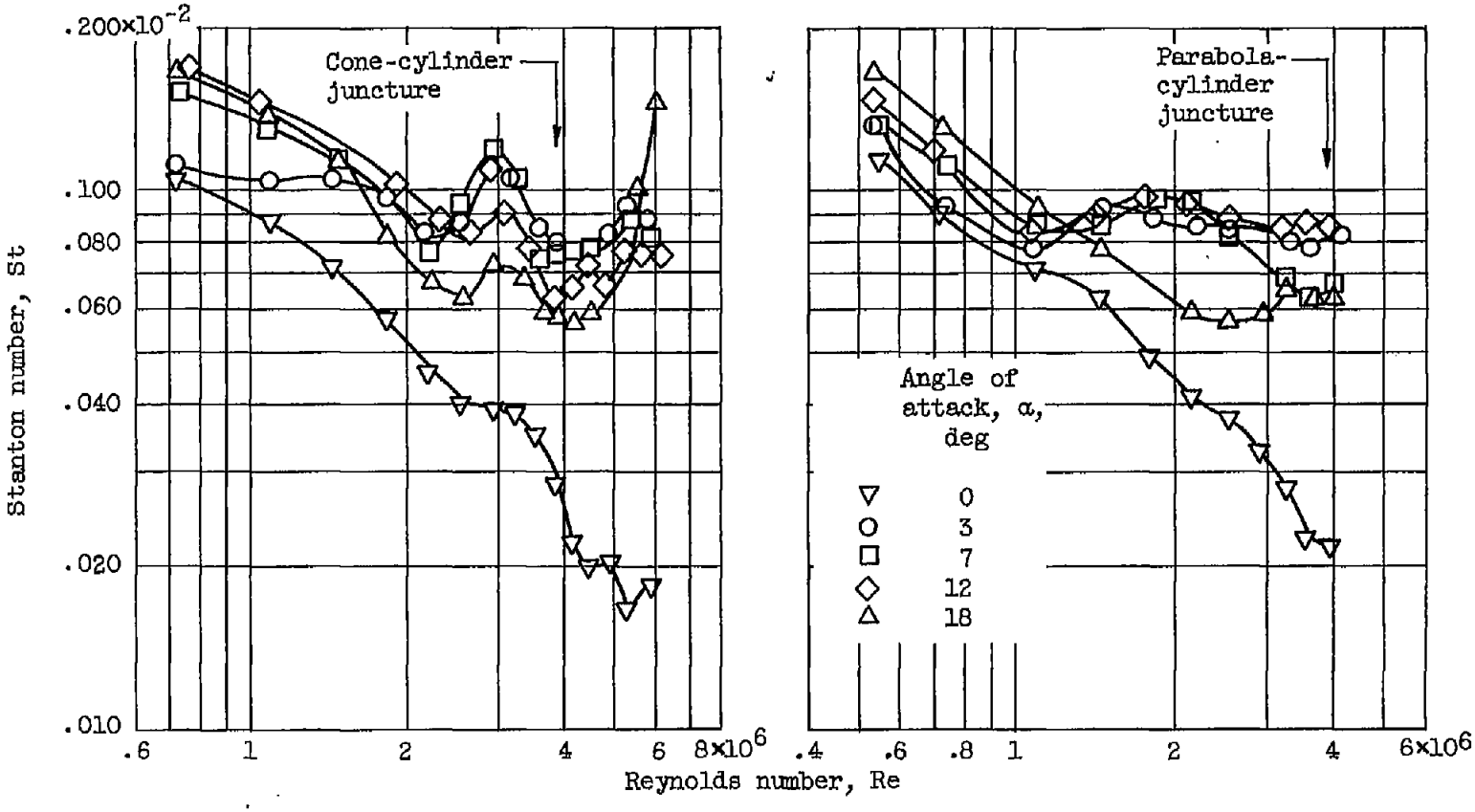

(a) Cone-cylinder model.

(b) Parabolic-nosed cylinder model.

Figure 6. - Effect of angle of attack on heat-transfer coefficient along the most leeward (180°) generator; unit Reynolds number per inch, 0.36×10^6.

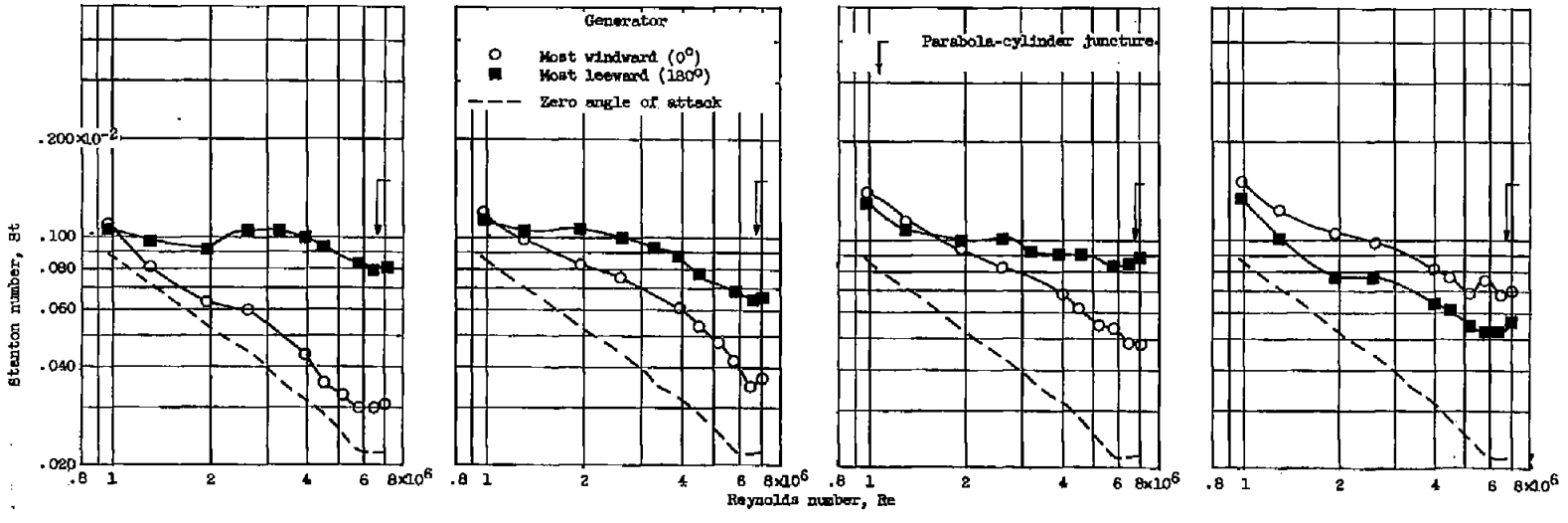

(a) Angle of attack, 3°. (b) Angle of attack, 7°. (c) Angle of attack, 12°. (d) Angle of attack, 18°.

Figure 7. - Comparison of Stanton numbers along the most windward (0°) and most leeward (180°) generators at various angles of attack; parabolic-nosed-cylinder model; unit Reynolds number per inch, 0.85×10^6.

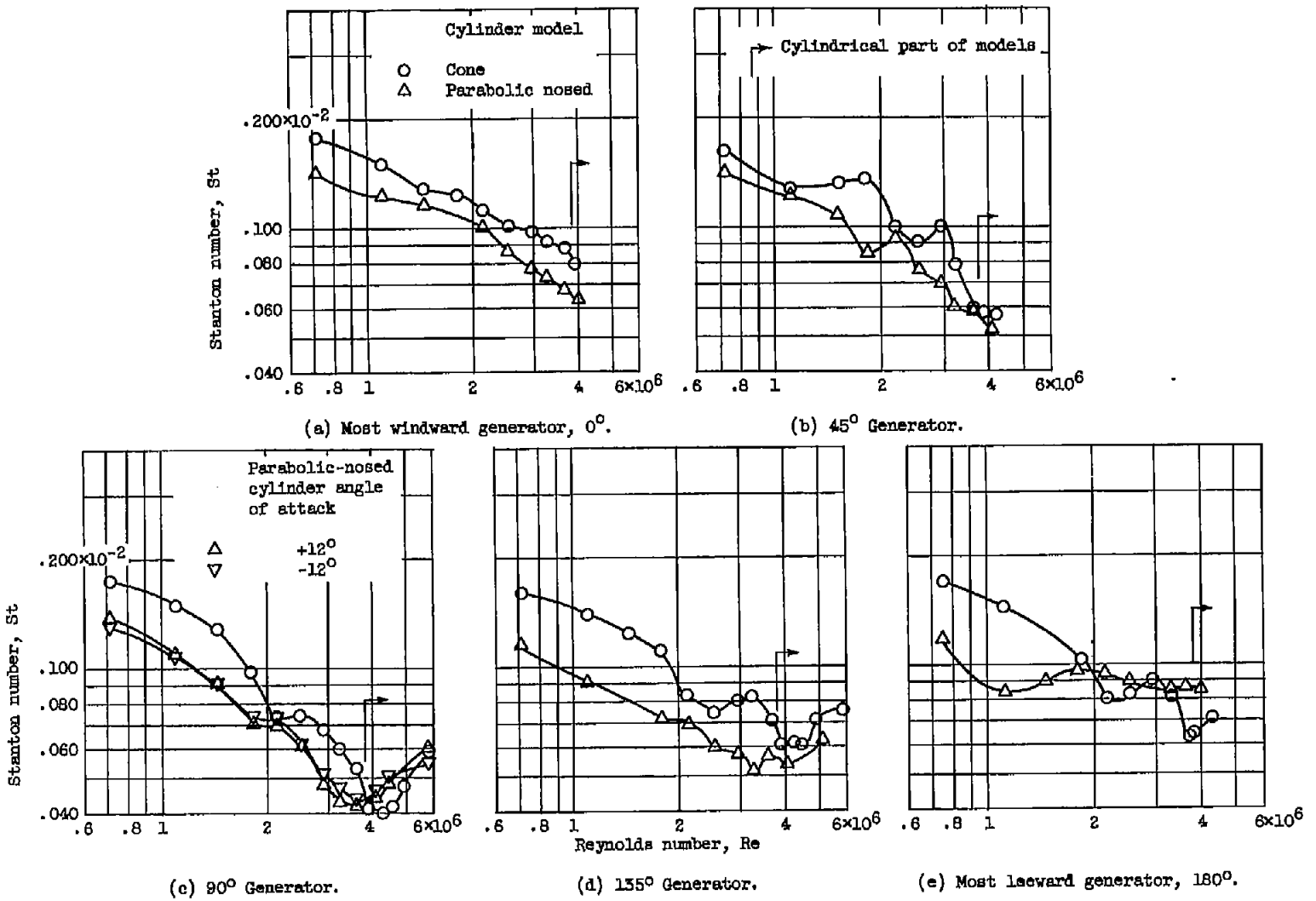

(a) Most windward generator, 0°.

(b) 45° Generator.

(c) 90° Generator.

(d) 135° Generator.

(e) Most leeward generator, 180°.

Figure 8. - Effect of forebody geometry on heat-transfer coefficient; angle of attack, 12°; unit Reynolds number per inch, 0.36×10^6.

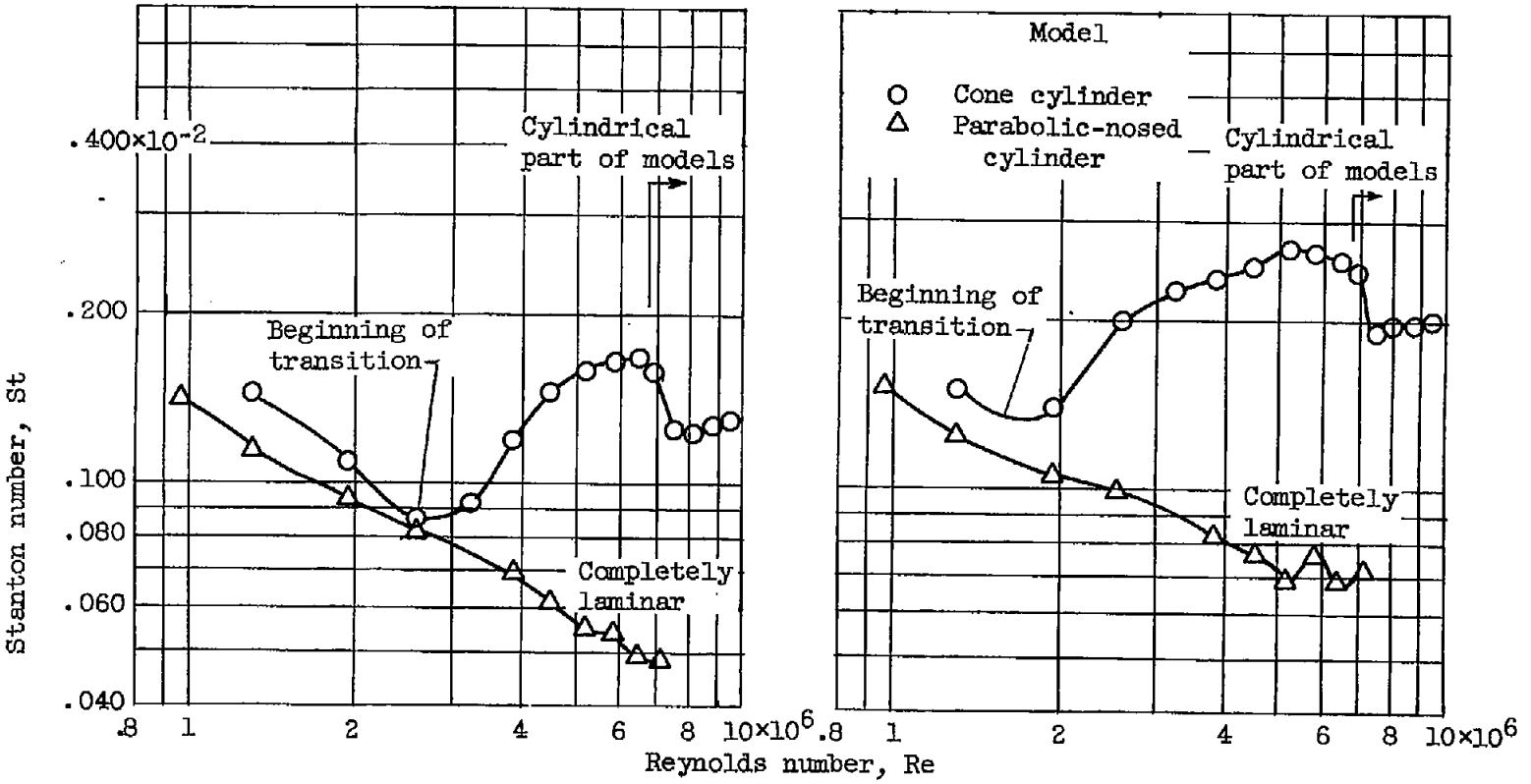

(a) Angle of attack, 12°.

(b) Angle of attack, 18°.

Figure 9. - Effect of forebody geometry on the location of transition to turbulent flow along the most windward generator; unit Reynolds number per inch, 0.65×10^6.

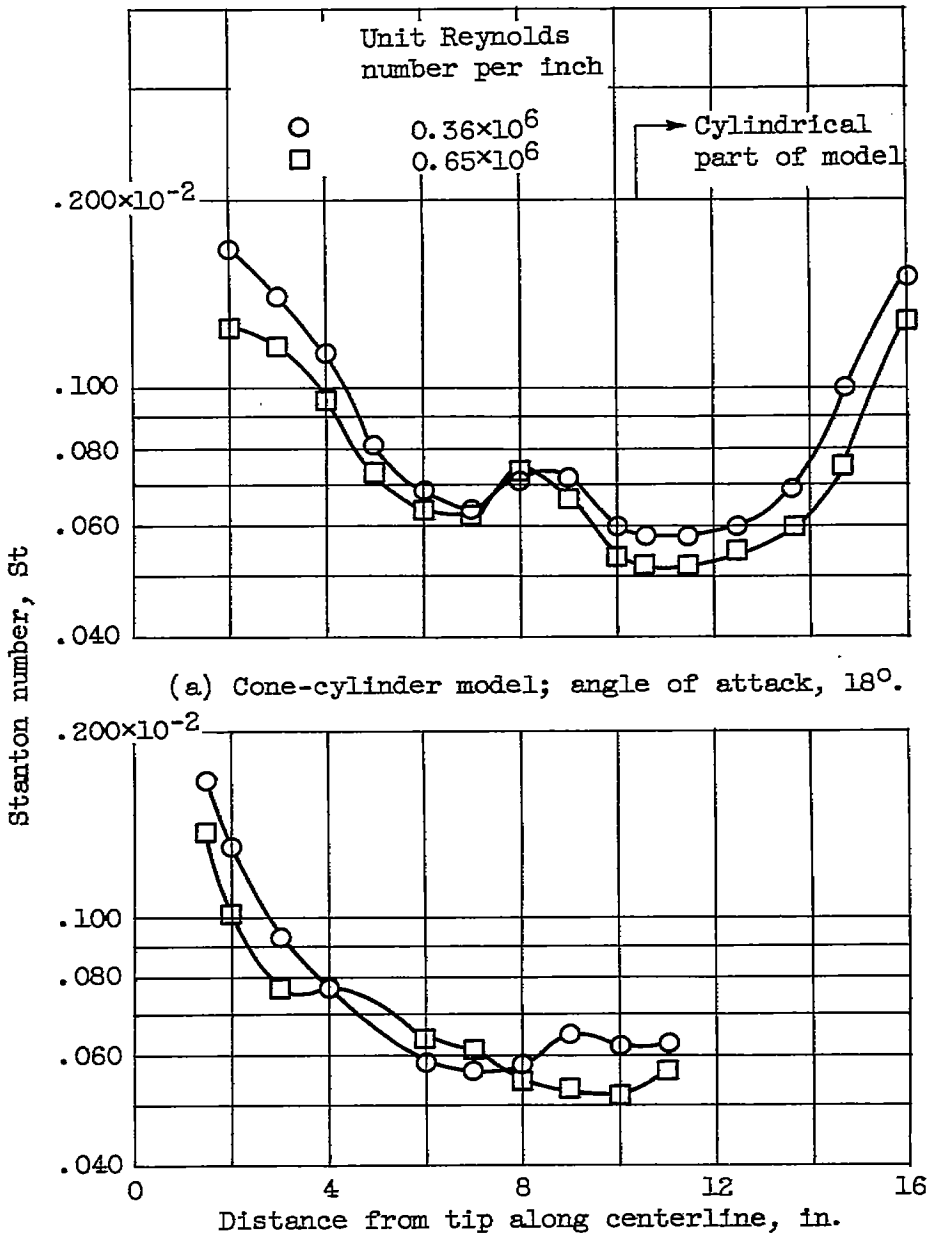

(a) Cone-cylinder model; angle of attack, 18°.

(b) Parabolic-nosed-cylinder model; angle of attack, 18°.

Figure 10. - Heat-transfer coefficients along the most leeward generator at two values of the unit Reynolds number.

NACA - Langley Field, Va.